10th Brazilian Congress on Computational Intelligence (CBIC'2011), November 8 to 11, 2011, Fortaleza, Ceará Brazil

A PARALLEL NEURAL SENSORLESS STRATEGY APPLIED TO THREE-PHASE INDUCTION MOTOR DRIVE

Tiago H. dos Santos[1], Alessandro Goedtel[1], Sergio A. Oliveira da Silva[1] and Marcelo Suetake[2]

[1] *Electrical Engineering Department, Federal Technological University of Paraná, Avenida Alberto Carazzai 1640, CEP 86300-000, Cornélio Procópio, PR, Brazil*

[2]*Electrical Engineering Department,* Engineering *School of São Carlos, University of São Paulo, Avenida do Trabalhador São-carlense 400, CEP 13566-590, São Carlos, SP, Brazil*

Emails: tiagohenrique.santos@gmail.com; agoedtel@utfpr.edu.br; augus@utfpr.edu.br; mclsuetake@usp.br

Abstract – This work proposes an artificial neural network approach to estimate the induction motor speed applied in a scalar drive. The induction motor has a great importance in many industrial sectors in which most control strategies are based on speed measurement of the motor axis. However, the direct measurement of this quantity reduces its robustness, compromises the driver system and control, besides increasing the implementation cost. The presented strategy estimates the induction motor speed when it is driven by semiconductor switch commanded by space vector pulse width modulation. Simulation results are presented to validate the performance of the proposed method under motor load torque variations.

Keywords – Induction motors, artificial neural networks, speed estimation, scalar control.

Resumo – Este trabalho propõe uma abordagem baseada em rede neural artificial para estimar a velocidade do motor de indução aplicado a um *driver* escalar. O motor de indução tem grande importância em muitos setores industriais e a maioria das estratégias de controle baseia-se na medição de velocidade do eixo do motor. Entretanto, a medição direta desta variável reduz sua robustez, comprometendo o sistema de acionamento e controle, além de aumentar o custo de implementação. A estratégia apresenta as estimativas de velocidade do motor quando este é acionado por chaves semicondutoras comandadas por modulação por largura de pulso *space vector*. Resultados de simulação são apresentados para verificar a performance do método proposto enquanto o motor de indução é submetido a variações de torque.

Palavras-chave – motor de indução, redes neurais artificiais, estimação de velocidade, controle escalar.

1 Introduction

Three-Phase Induction Motors (TIM) are used in many industrial sectors as leading element to convert electrical into mechanical energy. The main features are their low cost and robustness.

The applications that include TIMs can be divided into two groups: *i*) the induction motor is directly coupled to the power grid without control strategy; *ii*) the induction motor is driven by scalar or vector controls. For both groups, the determination of the machine speed by direct measurement or estimation methods is necessary in several industrial applications.

The motor speed can be measured with optical encoders, electromagnetic resolvers or brushless dc tachogenerators. However, the use of these eletromechanical devices present some limitations, such as the increasing driver costs, reduced mechanical robustness, low noise immunity, influence in the machine inertia and the requirement of a special attention with respect to these devices in hostile environments [1].

The use of sensorless technique is mainly found in high performance applications, such as vector-controlled and direct torque controlled drives. The main sensorless control strategies are based on open-loop estimators, e.g., the stator current and voltage monitoring, state observers, reference systems with adaptive models and estimator based on intelligent systems, such as Artificial Neural Network (ANN) and fuzzy logic [1].

Most speed estimators are obtained from the mathematical model of induction motor, which requires a precise knowledge of motor parameters [2]. Speed estimators based on State Observers (SO) need the exact values of the machine parameters for the correct operation of the sensorless device in low-speed regions [3]. This method also requires a considerable computer effort, since the algorithm of the estimator demands differential equations solving.

Recently, several methods for TIM speed estimation have been investigated [4-8]. In [4], a speed estimator based on sliding mode method is presented, where the machine parameters and the stator current are the model input.

In [5], an adaptive reference model for TIM speed estimation is used to speed estimation. The tuning of the reference model is accomplished by adjusting the parameters of the adaptive model aiming at the cancellation of error between the instantaneous reactive magnetizing power in the rotor and the estimated by the adaptive model.

A neural speed and rotor resistance estimator of a TIM using an Adaline network is presented in [6], in which the stator current and voltage are measured in the three-phase stationary reference frame (*abc*-axes). After the transformation from *abc*-axes to two-phase stationary frame ($\alpha\beta 0$-axes), the stator current and voltage are used to estimate the rotor current, rotor flux and derivative of the rotor flux, which are the inputs of the ANN. To validate the neural speed estimator, it is applied various TIM control strategies, such as scalar and vector controls. In [7], a strategy to estimate TIM rotor resistance using ANN is also presented, and its results are compared with a fuzzy logic-based estimator.

In [8], a TIM speed estimator based on Multilayer Perceptron Neural Network is also presented. The estimator inputs are the current and voltage on synchronous reference frame. In steady state, the training and validation data set of the neural speed estimator are acquired with the machine operating from 500 to 1000 revolution per minute (rpm) speed.

The proposal of this work is the development of a parallel neural speed estimator applied to a TIM fed by a non-sinusoidal power supply. It is driven by a Voltage Source Inverter (VSI) using scalar control. The input data of estimator, such as current, voltage and voltage-frequency are used to training and to validate the ANN. The training data are generated from the simulation of the mathematical model of the induction motor. The VSI is modulated by means of Space Vector Pulse Width Modulation (SVPWM) and controlled by scalar strategy. The network training is carried out in offline mode. In order to validate the proposed method, simulation data set is presented to the trained ANN and its response is compared to the model of the machine.

This work is organized as follow: Section 2 presents the main aspects of mathematical modeling of the induction motor, scalar control and SVPWM. In Section 3 the methodology of model data treatment is presented. Section 4 presents the principles associated with ANN. Section 5 shows the simulation and computational validation results of the proposed structure and in Section 6 the conclusions of this work are presented.

2 Modeling Aspects of Induction Motor and its Driver

The first step in a supervised training of an artificial neural network is to compile the input and output data set, which are used to adjust the internal parameters of the network. In this procedure, the network is exposed to data sequences that describe satisfactorily the behavior of the analyzed system [9].

To generate the training data set of induction motor, several simulations are executed using Matlab/Simulink software at different speed operating points. Figure 1 shows the block diagram which describes the inputs and outputs of the proposed model. The TIM is driven by a VSI with space vector pulse width modulation (SVPWM). The control strategy used the ratio voltage/frequency (*V/f*) (scalar control).

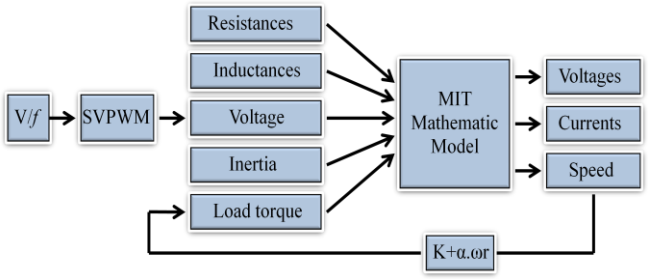

Figure 1 - Block diagram of system model.

A. Aspects of the TIM model

The induction motor model used in the simulations was developed in [10] and the machine parameters are obtained from a 4-pole motor, 220/380V, IP55 manufactured by WEG. Table 1 shows the parameters used in TIM simulations.

Table 1 - TIM Parameters

Standard Line – IV Pole – 60Hz – 220/380V	
Power	1 cv
Nominal current	3.018 A
Stator resistance	7.32 Ω
Rotor resistance	2.78 Ω
Stator inductance	8.95 mH
Rotor inductance	5.44 mH
Mutual inductance	0.141 H
Moment of Inertia	$2.71.10^{-3}$ kg.m²
Synchronous speed	188.49 rad/s
Slip	3.8%
Nominal torque	4.1 Nm

The voltage, current, voltage-frequency and the rotor speed are the quantities used in the neural network training process. In this study, linear loads, which are mainly found in fans, rolling mills, piston pumps and wood saw applications, were coupled on the rotor axis to evaluate the proposed method. These loads are featured by presenting a linear relationship between the load torque value and the rotor shaft speed [11].

B. The *V/f* control

The proposed methodology used for adjusting TIM speed consists in keeping the voltage-frequency (V/f) ratio constant, in order to maintain the magnetic flux in the air gap, which ensures proper operation of the machine. If the TIM voltage changes without the proper frequency adjustment, the machine can operate in the saturation region or the fluw field weakened [12]. The relationship between the TIM voltage source angular speed and synchronous speed is given by:

$$n_s = \frac{\omega_e}{P_p} \tag{1}$$

where n_s is the synchronous speed in radians per second (rad/s), ω_e is the stator flux angular speed (rad/s) and P_p is the pair of pole number.

The scalar control method is applied in TIM speed control by changing frequency and amplitude of the machine voltage, in order to maintain the maximum torque produced by the machine constant. Thus, the electromagnetic flux produced by TIM also remains constant. The electromotive force induced in the TIM air gap is described by (2).

$$E_l = 4.44 \cdot k_{\omega l} \cdot \Phi_m \cdot f \cdot N_l \tag{2}$$

where $k_{\omega l}$ is the stator winding factor, Φ_m is the maximum air gap flux, and N_l is the winding stator turns. The produced flux is calculated through the ratio between supply voltage and its frequency, as given by (3).

$$\Phi_m \cong \frac{V_f}{f} \cong K_{vf} \tag{3}$$

where K_{vf} is the proportionality constant between V_f and f.

The constant K_{vf} is also calculated through the peak voltage per phase V_{pf} and frequency f as presented in (4).

$$K_{vf} = \frac{V_{pf}}{f} = \frac{180}{60} = 3 \tag{4}$$

To calculate the constant K_{vf} in (4), the stator resistance losses and dc bus ripple were not considered. However, at low speed machine operation, such losses are increased, reducing the machine electromagnetic torque [13]. To minimize the voltage drop influence in stator resistance R_s, a voltage offset (V_{boost}) at the *V/f* is applied. V_{boost} is given by (5):

$$V_{boost} = R_s \cdot i_s \tag{5}$$

where the motor temperature variation was not taken into account.

Appling the parameters presented in Table I, V_{boost} can be calculated as follows:

$$V_{boost} = 3.23 \cdot 3.018 = 22.09V \tag{6}$$

Thus, the new gain K_{vf} is determined by:

$$K_{vf\_svpwm} = \frac{V_{pf} - V_{boost}}{f} = \frac{157.91}{60} = 2.63 \tag{7}$$

C. Driver SVPWM

The space vector pulse width modulation (SVPWM) has been widely applied in VSI. This technique has some advantages over the sinusoidal modulation, such as reducing the number of switching, reducing the harmonic content and higher modulation index [14]. In this work, the studied SVPWM is based on the model described in [15]. The SVPWM is applied to a three-phase VSI three-wire as shown in Figure 2, where S1 to S6 are the power switches.

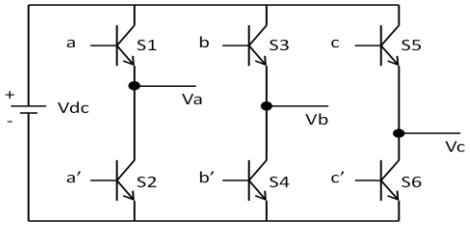

Figure 2 - Three-phase voltage source inverter.

The period that power switches remain in opened or closed state is used to determine the output voltage on the VSI. Through the analysis of Figure 3, the space vector modulation can be implemented by following three steps, namely: *i*) Determining the voltage vectors on the coordinate stationary $\alpha\beta 0$ axes (V_α and V_β), the reference voltage vector V_{ref} and the angle θ between V_{ref} and V_α; *ii*) Determining the times t_1 and t_2, which are the times of application of the vectors V_1 and V_2, respectively *iii*) Determining the conduction time of each switch (S1 , S2 and S3).

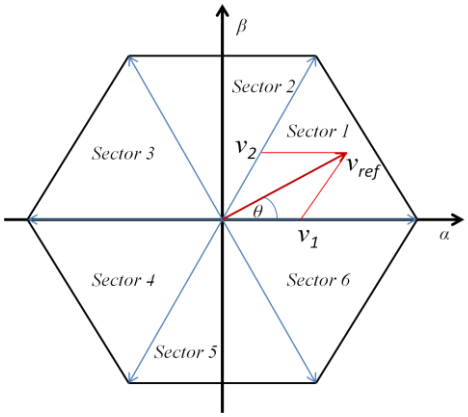

Figure 3 - Voltage output space in the $\alpha\beta$ coordinate system.

3 Data Processing Model

The voltage supplied by the inverter has a switching characteristic, which passes through the low-pass filter (LPF) before being processed in the PLL (Phase Locked Loop) system. Although the electric currents are naturally filtered, due to the inductive characteristic of the machine, the same LPF is used, in order to obtain high frequency noise attenuation and provide the similar phase displacement compared with voltage signal. In applications where variable speed control is needed, the TIM is usually driven by a VSI. The estimated machine speed through primary quantity, such as current and voltage, leads to the increasing cost of drivers with their transducers. However, this cost is lower compared to the direct speed measurement through sensors such as optical and tachogenerator.

In order to obtain the input patterns of the rotor speed function, stator voltage and current on synchronous reference frame *dq0* were used. Furthermore, the voltage-frequency ratio is obtained using a PLL system. Since the machine is considered a balanced load to the VSI, its currents are also balanced. Thus, by currents measurement of phase *a* and *b*, the phase *c* current can be directly calculated. Likewise, the line voltages v_{ab}, v_{bc}, v_{ca}. are obtained. Figure 4 presents the block diagram of the voltages and currents data treatment system.

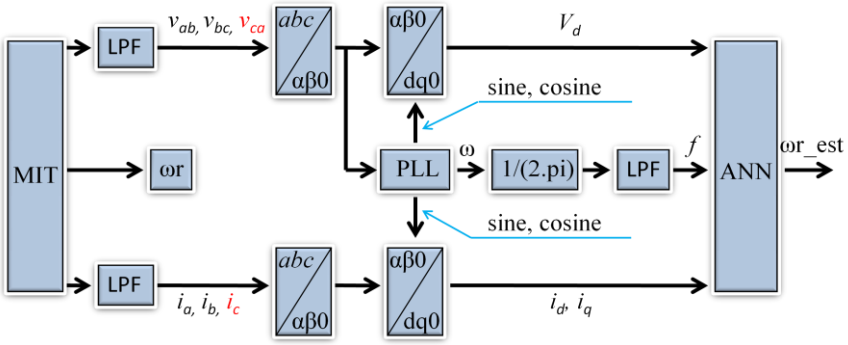

Figure 4 – Block diagram of the data processing.

The PLL system used in this paper is based on the single phase p-PLL algorithm described in [16]. Based on the three-phase instantaneous active power theory, the PLL system is developed in the two-phase stationary reference coordinate system ($\alpha\beta$ coordinates). The three-phase instantaneous active power can be represented into two forms, such as two-phase or three-phase, both in the stationary reference frame, as follow:

$$p = v_a \cdot i_a + v_b \cdot i_b + v_c \cdot i_c = v_\alpha \cdot i_\alpha + v_\beta \cdot i_\beta = \bar{p} + \tilde{p} \tag{8}$$

where the dc and ac components of the real power *p* are represented by $\bar{p}$ and $\tilde{p}$, respectively.

The implemented three-phase PLL is showed in Figure 5. The PLL structure operates to cancel the component $\bar{p}$ of the fictitious instantaneous power *p'*. Thus, when the average value of portion *p'* is zero, the output signal is locked with the fundamental component of input signal. The dynamics behavior of the PLL is defined by PI controller output, which provides the reference angular frequency ($\omega=2\pi f$), where *f* is the frequency of the input signal fundamental component.

The angle $\theta=\omega.t$ is obtained by integrating the angular frequency ω. Therefore, θ is used to calculate the fictitious current i'_α and i'_β. To cancel the *dc* component of the p' the fictitious current i'_α and i'_β must be orthogonal to the voltages V_α and V_β respectively [17].

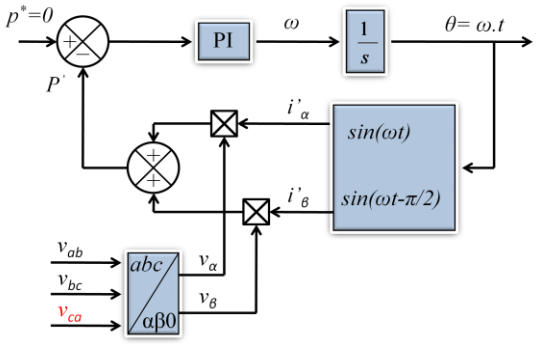

Figure 5 - Three-phase p-PLL system control.

Due to the dynamic response of the PI controller used in the PLL system, it is used a low-pass filter (LPF) to obtain a noise attenuation of the voltage-frequency. Likewise, low-pass filters are used in voltage and current measurement.

4 Neural Speed Estimator

The Artificial Neural Network (ANN) has proved to be efficient in various engineering problems. In this paper the ANN is applied as a universal function approximator in order to estimate induction motor rotor speed driven by a VSI with SVPWM. The used neural network is the multilayer perceptron with supervised training.

In this paper, four ANN are trained through an offline manner using data gathered from simulation and subsequent treatment. Each ANN is trained to act in an region of the *V/f* control and the operating range of each ANN and its configurations is presented in Table 2. For all ANN, the activation function of the hidden layers is the hyperbolic tangent, while the activation function of the output layers is the linear.

Table 2 - ANN structures and operating range

ANN	Number of Neuron			Operating range (Hz)
	First hiden layer	Second hiden layer	Output layer	
1	6	21	1	0-20
2	11	21	1	20-35
3	17	21	1	35-48
4	17	21	1	48-60

The artificial neuron presented in Figure 6 can be modeled mathematically as follows:

$$v_j(k) = \sum_{i=1}^{m} X_i.w_i + b \tag{9}$$

$$y_j(k) = \varphi(v_j(k)) \tag{10}$$

where $y_j(k)$ is the output signal of the *j*-th neuron with respect to instant *k*; w_i is the weight associated with the *i*-th input signal; X_i is the *i*-th input signal of the neuron; *n* is the number of input signal of the neuron; *b* is the threshold response associated with the neuron; $v_j(k)$ is the summing junction of the *j*-th neuron with respect to the instant *k* and $\varphi_j(.)$ is the activation signal of the *j*-th neuron.

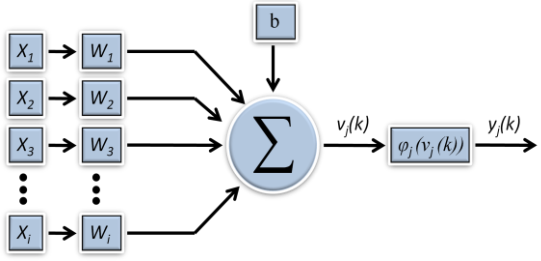

Figure 6 - Artificial neuron.

For each input signal, the artificial neuron is able to compute its output. In the training process, the adjustment of neural weights (w_i), associated to the *j*-th output neuron, is done by calculating the error $e_i(k)$ between the desired response and the response estimated in relation to the *k*-th iteration or input vector. The output error is calculated as follows:

$$e_j(k) = d_j(k) - y_j(k) \tag{11}$$

where $d_j(k)$ is the desired response to the *j*-th output neuron. Adding all square errors produced by the output neurons of the network concerning to *k*-th iteration results in (12):

$$E(k) = \frac{1}{2}\sum_{j=1}^{p} e_j^2(k) \tag{12}$$

where *p* is the number of output neuron.

For an optimum weight configuration, $E(k)$ is minimized with respect to the synaptic weight w_{ji}. Therefore, the weights associated with the output layer of the network are updated using the following relationship:

$$w_{ji}(k+1) = w_{ji}(k) - \eta \frac{\partial E(k)}{\partial w_{ji}(k)} \tag{13}$$

where η is a constant that determines the learning rate of the backpropagation; w_{ji} is the weight connecting the *j*-th neuron of the output layer to *i*-th neuron of the previous layer. The adjust of weights belonging to the hidden layers of the network is carried out in an analogous way. The weights adjust process is detailed in [18].

The proposed estimator in this paper is structured as shown in Figure 7. The voltage, current and the frequency are presented to the ANN after processing the simulation data, where output is the speed estimated, used in training and validation process. The ANN to be used in the validation and operation is chosen by voltage level.

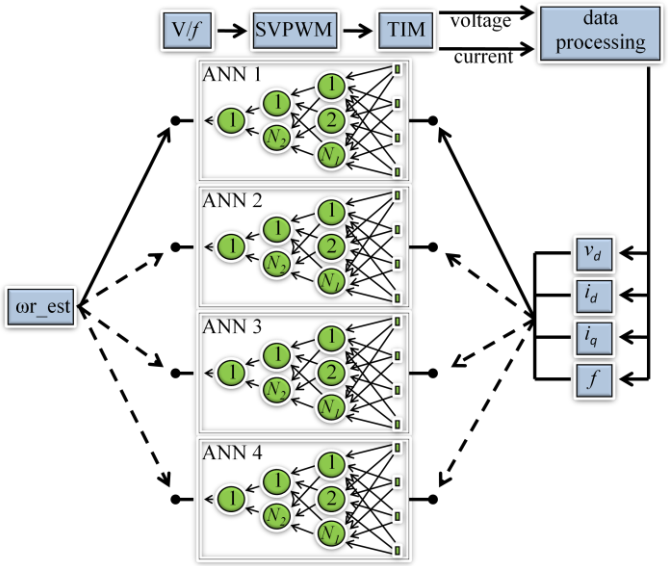

Figure 7 - Training and ANN test structure.

To optimize the neural network training, a learning reinforcement process was applied in low speed regions. Therefore, data set which represents various aspects of the system dynamic in all operating domain is presented.

5 Generalization Results

The ANN was trained from the data obtained from computer simulations of TIM operating under scalar control in several operation points. Table 3 presents four speed region simulations, each one associated with an ANN.

Table 3 - TIM operation point

Simulation number	Voltage frequency (Hz)	Synchronous speed (rad/s)
1	5	15.708
2	25	78.539
3	44	138.230
4	56	175.929

For the simulation it was considered the linear torque load in the following form:

$$T_l = k_t + \alpha.\omega_r \tag{14}$$

where T_l is the torque load, k_t is the initial torque load constant in N.m, α is the constant of relation torque/speed given by N.m/rad/s and ω_r is the TIM rotor speed. In all simulations, it is considered the torque constant (k_t) with a value of 0.1 N.m and a load with inertial moment of $2.71.10^{-3}$ kg.m². In order to validate the ANN it is applied a step load torque in the machine as presented in Figure 8-11.

Figure 8 presents the generalization results of the parallel neural estimator. Simulation 1 (Table 3) takes into consideration the starting dynamics to steady state of the TIM at low speed (Figure 8a). The simulation is performed with a sample rate of 6k samples/s. Following the same simulation methodology, the Figure 8b and 8c show the dynamic response of estimator using the ANN 2 and ANN 3 for simulation 2 and 3 respectively. The increase of oscillation of the estimated speed during machine acceleration is due to low load torque in this operating point. During this period there is an oscillation of the electromagnetic torque produced by the machine, which is also reflected in the currents i_d and i_q. The estimated speed showed in Figure 8d also has oscillatory characteristics in acceleration period similarly with the estimated speed in Figure 8c.

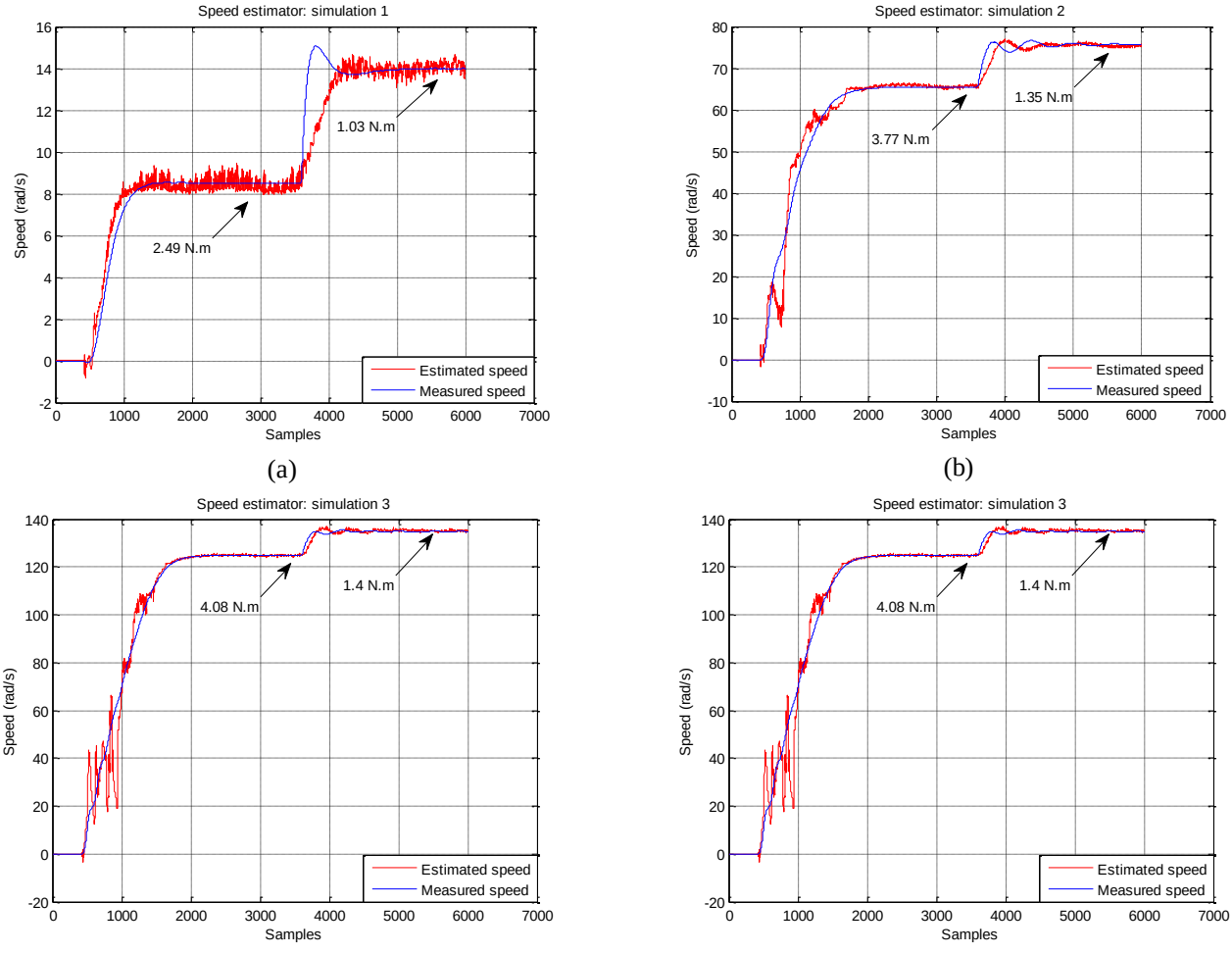

Figure 8 - Generalization results: (a) Simulation 1, (b) Simulation 2, (c) Simulation 3, (d) Simulation 4.

The relative mean error produced by the speed estimators in relation with each simulation model is presented in Table 4.

Table 4 - Relative mean error of the proposed estimator

Simulation	Relative Mean Square Error (%)
1	6.100
2	3.370
3	2.824
4	2.119

Simulations results demonstrate the ability of each ANN separately estimate the TIM speed in the transitory and steady state drived by scalar control even in low speed region.

6 Conclusions

This work proposed an alternative methodology to estimate the induction motor speed driven by a VSI with scalar control, based on four parallel artificial neural networks with supervised training process in off-line mode. The ANN selection was made through voltage range operations.

The methodology was applied to estimate the motor speed during transient and steady state, comprising the whole operation range of the scalar control, including the regions of very low speed. In each simulation it was applied a load torque variation when the TIM was operating in steady state, with the aim of analyzing the robustness of the proposed method. Simulation results presented lower mean relative average errors achieved for all speed operating ranges. Besides, the proposal can be applied to other methods of speed control or parameter estimator of induction motor using the ANN.

Ackmowledgment

The authors gratefully acknowledge the financial support under grand 474290/2008-5, nº 471825/2009-5 received from CNPq and process nº 06/56093-3 received of Araucária Fundation and CAPES.

7 References

[1] P. Vas, Sensorless Vector and Learning Machines, **Oxford University Press**, (1998).

[2] V. Vasic. S. N. Vukosavic, E. Levi, A stator resistence estimator scheme for speed sensorless rotor flux oriented inductor motor drivers, **IEEE transactions on Energy Conversion**, 17 (2003), 476-483.

[3] B. K. Bose, Modern Power Eletronics and AC Drives, **Prentice Hall**, (2002).

[4] M. Comanescu, An inductor-motor speed estimator based on integral sliding-mode current control, **Prentice Hall**, (2009).

[5] J. R. Jevremovic, V. Vasic, D. P. Jeftenic, Speed-sensorless control of induction motor based on reactive power with rotor time constant identification, **Electric Power Application (IET)**, 4 (2010), 462-473.

[6] I. M. Mostafa, F. S. Mostafa, A. E. Ahmed, A speed estimator unit for induction motors based on adaptive linear combiner, **Elsevier Energy Conversion and Manangement**, 50 (2009), 1664-1670.

[7] P. F H. González, J. J. R. Rivas, I. C. T. Rodríguez, Rotor Resistance Estimation using a Artificial Neural Network into the Indirect Vectorial control of the Induction Motor (*in spanish*), **IEEE Latin America Transaction**, 6 (2008), 176-183.

[8] O. Yuksel, D. Mehmet, Speed estimation of vector controlled squirrel cage asynchronous motor with artificial neural network, **Elsevier Energy Conversion and Manangement**, 52 (2009), 675-686.

[9] A. Goedtel, I. N. da Silva, P. J. Serni, C. F. Souza, Neural structure for speed estimator of three-phase induction motors based on experimental and simulations data (*in portuguese*), **Simpósio Brasileiro de Automação Inteligente (SBAI)**, (2007).

[10] C. M. Ong, Dynamic Simulation of Electric Machinery Using Matlab/Simulink. **Prentice Hall**, (1998).

[11] L. P. C. Dias, O. S. Lobosco, Electric Motors: Selection and Application, **McGraw-Hill Inc.**, (1998).

[12] M. Suetake, I. N. da Silva, A. Goedtel, DSP Embedded Compact Fuzzy System and its Application to V/F Control of induction (in portuguese), **Revista Controle & Automação**, 21 (2010), 245-259.

[13] R. Krishnan, Electric Motors Drivers: Modeling, Analysis, and Control, **Prentice Hall**, (2002).

[14] H. Pinheiro, F. Botterón, Space Vector modulation for Voltage Source Inverter: A Unified Approach (*in portuguese*), **Revista Controle & Automação**, 16 (2005), 13-24.

[15] H. W. Broeck, H. C. Skudelny, G. V. Stanke, Analysis and Realization of a Pulsewidth Modulator Based on Voltage Space Vector, **IEEE Transactions on Industry Applications**, 4 (1988), 142-150.

[16] S. A. O. Silva, L. B. G. Campanhol, A. Goedtel, A comparative Analysis of p-PLL Algorithms for Single-Phase Utility Connected Systems, **IEEE European Power Electronics Conference and Applications (EPE)**, (2009).

[17] S. A. O. Silva, R. Novochadlo, R. and Modesto, Single-phase PLL structure using modified p-q theory for utility connected systems, **in Proceeding of Brazilian Power Electronics Conference (PESC)**, 4706-4711, (2008)

[18] .S. Haykin, Neural Networks and Learning Machines, **Prentice Hall**, (2008).